Acta Cryst. (1991). A47, 74-82

Brillouin Zones and Kikuchi Lines for Crystals Under Electron Channeling Conditions

BY M. GAJDARDZISKA-JOSIFOVSKA AND J. M. COWLEY

Department of Physics, Arizona State University, Tempe, AZ 85287-1504, *USA*

(*Received* 5 *March* 1990; *accepted* 4 *September* 1990)

Abstract

The geometry of the Kikuchi lines in high- and low-energy electron diffraction patterns is defined in terms of intersections of the Brillouin zone boundaries with a sphere of reflections. Full treatment of the cases of two-dimensional and one-dimensional real lattices reveals previously unknown boundaries in the form of parabolic surfaces (2D) and paraboloids of revolution (1D). These boundaries are applied to K lines which arise from electron channeling. Correlation is made with the previous explanations of parabolas and circles in the reflection high-energy electron diffraction (RHEED) and transmission high-energy electron diffraction (THEED) patterns and $K2$ and $K1$ lines in low-energy electron diffraction (LEED) patterns. Experimental convergent-beam RHEED patterns of a reconstructed MgO (111) surface are presented in which parabolas due to the surface periodicity are shown for the first time.

1. Introduction

It is well known that Kikuchi bands and lines, as well as parabolas and circles, can be observed in the high-energy electron diffraction patterns from electron transparent crystals (transmission high-energy electron diffraction: THEED), and from surfaces of bulk crystals (reflection high-energy electron diffraction: RHEED). The parabolas and the circles are more prominent in the RHEED patterns and have regained attention due to their association with surface channeling (resonance) effects. Their geometry has been described in several works (Ichimiya, Kambe & Lehmpfuhl, 1980; Lehmpfuhl & Dowell, 1986; Peng & Cowley, 1987; Yao & Cowley, 1989; Gajdardziska-Josifovska & Cowley, 1989) but is still the subject of discussion. The parabolas and circles in the transmission patterns have only recently been compared to their surface equivalents (Lehmpfuhl & Dowell, 1986; Yao & Cowley, 1989; James, Bird & Wright, 1989) to suggest that they should also be connected with electron channeling.

Lines, other than the conventional Kikuchi lines, have also been observed in the low-energy electron diffraction (LEED) patterns from surfaces of single crystals. They have been called $K2$ and $K1$ lines and have been ascribed to diffraction from the two-dimensional surface and the one-dimensional rows of atoms on the surface (De Bersuder, 1968). $K2$ lines have also been related to the surface resonance effects (*e.g.* McRae, 1979).

Miyake & Hayakawa (1970) have pointed out that the surface resonance effects in LEED should be equivalent to the surface channeling effects in RHEED (also known as the second kind of intensity anomaly). Chadderton (1970) has argued that electron channeling effects should be described in the framework of wave mechanics and are essentially diffraction phenomena (exceptions are very high-energy electrons whose channeling resembles the classical channeling of ions).

This paper is an attempt to unify the numerous previous observations and descriptions of the different lines in the THEED, RHEED and LEED patterns. We will demonstrate that Brillouin zones can be used to reproduce the geometry of the lines seen in the diffraction patterns, and to gain insight into their physical meaning. We will consider three-dimensional (3D), two-dimensional (2D) and one-dimensional (1D) real lattices and give full treatment of their Brillouin zone boundaries. Emphasis will be given to the boundaries which, to our knowledge, have not been described before. We use those boundaries to explain the channeling geometries both in the bulk and at the surface of crystals. We also show experimental RHEED patterns from a reconstructed MgO (111) surface in which parabolas due to the surface periodicity are observed for the first time. This experimental result supports our general conclusion that the dimensionality of the periodic scattering object determines the geometry of the Kikuchi pattern, and that channeling only serves to reduce the effective dimensions of the 3D crystals.

2. Brillouin zones and Kikuchi lines of crystals

2.1. *Brillouin zones and diffraction*

The Brillouin zones (BZ) are among the basic concepts of solid-state physics. Even though their construction exhibits all the incident wavevectors which can be Bragg scattered by the crystal, the zones have seldomly been used when describing electron diffraction. In this section we will give a brief review of the diffraction condition for a periodic lattice of scatterers, and of the Brillouin construction as its geometrical representation. The purpose of the review

0108-7673/91/020074-09$03.00

is to introduce the notation and the conventions which will be used in the subsequent sections.

Conservation of energy in the elastic scattering events imposes equality of the magnitudes of the incident wavevector ($\mathbf{k}_0$) and the scattered wavevector ($\mathbf{k}$): $k_0^2 = k^2$. Conservation of momentum requires that the scattering vector ($\Delta\mathbf{k}$) be a vector of the reciprocal lattice ($\mathbf{g}$): $\Delta\mathbf{k} = \mathbf{k} - \mathbf{k}_0 = \mathbf{g}$. The combination of the two equations gives the diffraction condition

$$2\mathbf{k}_0 \cdot \mathbf{g} + g^2 = 0 \qquad (1)$$

which can be rewritten as

$$\mathbf{k}_0 \cdot (-\mathbf{g}/2) = (g/2)^2. \qquad (1a)$$

The geometrical interpretation of (1*a*) gives the Brillouin construction. Namely, when one point of the reciprocal lattice is chosen as its origin, and the reciprocal-lattice vector ($-\mathbf{g}$) is bisected by a perpendicular plane, then any incident wavevector which starts at the origin and ends on the plane will satisfy the diffraction condition [the convention used by Kittel (1976) is followed for the direction of $\mathbf{k}_0$]. The procedure is repeated for all the reciprocal-lattice vectors and the obtained planes form the boundaries of the Brillouin zones. They specify all the energies and directions of the incident waves which can be diffracted by the periodic lattice of scatterers.

An example of the Brillouin construction is given in Fig. 1 for a ⟨001⟩ projection of a cubic reciprocal lattice. Note that this construction is done with respect to the reciprocal lattice which is fixed to the real lattice. Hence, the Brillouin zone boundaries do not depend on the incident-beam direction and move only when the real lattice is tilted.

2.2. *Kikuchi lines of crystals (3D real lattices)*

The geometry of the Brillouin zone boundaries of Fig. 1 resembles the geometry of the Kikuchi lines which are observed in the high-energy electron diffraction (HEED) patterns. The Kikuchi lines are due to electrons which have been scattered diffusely or inelastically within the crystal. The forward peaked spherical electron waves, which arise from the different nonelastic events, are incoherent with each other and with the incident beam. However, each of those beams is coherent with itself, and is subject to elastic scattering by the crystal (*e.g.* Cowley, 1984; Fan, 1989). The role of each primary diffuse or inelastic scattering event is to expose the crystal to a wide-angle coherent illumination.

In the geometrical construction we represent the spherical coherent illumination by a sphere of radius $k_0 = 1/\lambda$ which is *centered at the origin of the reciprocal lattice of the crystal* and is filled with incident wavevectors. The reciprocal-lattice origin is then translated to the surface of the sphere and positioned at the ends of each of the incident wavevectors. In the following discussion we will refer to this sphere as the 'sphere of reflections', but we want to note that it is in essence an Ewald sphere with two additions to the standard convention. Namely, for parallel illumination the only difference is that we introduce an additional reciprocal lattice whose origin is at the center of the Ewald sphere and with respect to which we draw the Brillouin zone boundaries. The condition for diffraction is again satisfied when a point of the reciprocal lattice (fixed to the end of the incident wavevector) lies on the surface of the Ewald sphere, but from Fig. 1 it is obvious that we can rephrase this clause by saying that diffraction occurs from a given crystal plane when the incident wavevector ends on one of the BZ boundaries constructed by bisecting the reciprocal-lattice vectors of that plane.

The second more-important difference between the standard Ewald-sphere construction and the one proposed here stems from the convention that we introduced to represent wide-angle illumination. The usual convention is to have only one reciprocal lattice with a different Ewald sphere for each direction of incidence [an example is given in Fig. 2(*a*) for a convergent-beam diffraction]. This description is correct, but it does not correspond in a straightforward

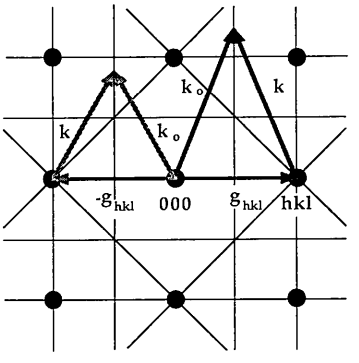

Fig. 1. Brillouin zone boundaries are constructed by bisecting every reciprocal-lattice vector $\mathbf{g}_{hkl}$ with an orthogonal plane, as shown for the (001) reciprocal-lattice plane of a cubic lattice. The incident wavevector $\mathbf{k}_0$ which starts at the origin and ends on one of those planes satisfies the conditions for elastic scattering.

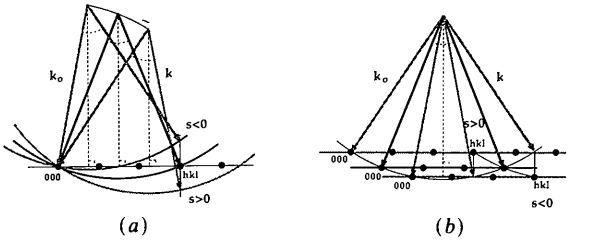

Fig. 2. Two equivalent Ewald-sphere constructions for convergent-beam illumination. (*a*) The conventional representation with one reciprocal lattice and a range of spheres. (*b*) Representation with one sphere and a range of reciprocal lattices which corresponds directly to the experimental geometry.

manner to the experimentally observed diffraction geometry. For example, the impression from Fig. 2(*a*) is that the Laue circles (the intersections of the Ewald spheres with the reciprocal-lattice plane) are not concentric, while in the experimental convergent-beam electron diffraction (CBED) patterns they are concentric (Spence, 1990) and their centers are on the zone axis (Gajdardziska-Josifovska & Cowley, 1989). To derive these conclusions one would need to consider that all the parallel directions meet at a point at infinity (or in the back focal plane of the objective lens in a transmission electron microscope). Thus, the centers of the Laue circles, which in Fig. 2(*a*) are obtained by projecting the centers of the Ewald spheres onto the zero-order Laue zone, merge to a point in the diffraction pattern because the projecting lines are parallel to each other and to the zone axis of the particular zero-order Laue zone. To avoid this convoluted thinking imposed by the standard convention of one reciprocal lattice with many Ewald spheres, we propose a convention in which the wide-angle illumination is represented by one sphere with many reciprocal lattices (Fig. 2*b*). This geometry corresponds directly to the geometry of the experimental diffraction patterns (*e.g.* the diffraction spots are discs with diameter defined by the convergence angle; all the points in the transmitted disc are 000 points; the Laue circles are concentric; the excitation error is positive for the inner half of the excited disc but negative for the outer half; ...), but even though it is instructive for convergent-beam patterns, it would be very cumbersome for spherical illumination. In the latter case the convergence angle is 2π and if the scattering geometry is to be deduced by the sole use of the Ewald-sphere-type construction, one would need to draw an infinite number of reciprocal-lattice planes and keep track of each of their origins (or infinite number of spheres in the standard convention). The problem is simplified by combining the sphere of reflections (Fig. 2*b*) with the Brillouin zone boundaries (Fig. 1). In this case all the possible directions for elastic scattering are defined by the intersections of the sphere with the BZ boundaries (*i.e.* draw a sphere of radius k_0 which is centered at the origin in Fig. 1 and note that the Bragg condition is satisfied only when the incident beam ends on one of the intersections of the BZ boundaries with the sphere). In the diffraction pattern these directions correspond to the experimentally observed Kikuchi lines. This description can also be applied to the Kossel lines in the X-ray patterns, the Kossel patterns in the convergent-beam electron diffraction, and the Kossel–Möllenstedt patterns in the shadow images of crystals. In the subsequent sections we will refer to all these lines when speaking about Kikuchi lines, and will call them *K* lines.

An example of the above description for the geometry of the *K* lines is given in Fig. 3 where one plane of the Brillouin zones is intersected with a sphere of reflections. The allowed directions for elastic scattering form a cone whose semiapex angle $(90°-\Theta)$ depends on the length of the reciprocal-lattice vector giving the plane (g_{hkl}) and on the radius of the sphere ($1/\lambda$). The simple derivation $\cos(90°-\Theta)=(g_{hkl}/2)/(1/\lambda)$ gives the Bragg law for the (*hkl*) crystal plane: $2d_{hkl}\sin\Theta=\lambda$. A similar construction is described by Hirsch, Howie, Nicholson, Pashley & Whelan (1977) but their sphere is of radius $2/\lambda$. The intersection of the cone with the diffraction screen will define the geometry of the experimentally observed *K* line. In the HEED configuration, the screen is flat and the intersection is a hyperbola. Owing to the small scattering angles, the hyperbola is approximated with a straight line for all the practical considerations of *K* lines. In the LEED configuration the screen is hemispherical and the intersection of the cone with it gives a *K* line in the form of a circle or a segment of circle.

All the *K* lines can be obtained by considering the cones which arise from all the Brillouin zone boundaries of the 3D crystal. Since the Brillouin zones are fixed to the crystal, the *K* lines give direct information about the orientation of the crystal. The intensity of the Kikuchi lines is a much more involved subject, and is beyond the scope of this work.

3. Brillouin zones of 2D real lattices

3.1. *Constructions and general properties*

The reciprocal lattice of a 2D real lattice is made of infinite rods which are parallel to each other and are orthogonal to the plane of the real lattice. A top view of a simple square reciprocal lattice looks the same as that of a 3D lattice (Fig. 1). The BZ boundaries in this plane of the projection are the conventional ones for 2D lattices. For their construction it is sufficient to treat the reciprocal lattice as a 2D

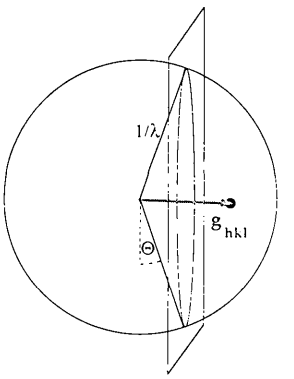

Fig. 3. The intersection of the sphere of reflections with the plane which is a normal bisector of the reciprocal-lattice vector $\mathbf{g}_{hkl}$ gives a circle. The wavevectors which start at the center of the sphere and end on the intersecting circle form a cone which yields a Kikuchi line of the (*hkl*) plane.

lattice made of points. These boundaries describe the possible directions for elastic scattering within the plane of the real lattice (when both the incident and the scattered wavevectors are parallel to this plane).

This standard description of the BZ boundaries of 2D real lattices falls short of recognizing the 3D nature of the reciprocal lattice. Because of that it does not describe the elastic scattering events in which the incident or the scattered wavevector is at an angle to the real lattice. The same lack of full description was also found for the 1D case. We aim to fill the gap in this paper.

If the reciprocal lattice is observed edge on, as in Fig. 4, the rods become apparent. One point on a rod is chosen as an origin of the reciprocal lattice, and the lattice is characterized by continuous sets of reciprocal vectors. Each reciprocal vector should then be bisected by an orthogonal plane to obtain all the possible BZ boundaries.

Let us first discuss the boundaries arising from the rod that contains the origin of the reciprocal space (Fig. 4*a*). Since the rod describes a continuum of reciprocal vectors we can choose a vector with an arbitrary length and bisect it. The resulting plane gives geometrical representation of reflection from the 2D lattice. Namely, when the incident wavevector ends on any point of this plane, its tangential component is equal to the tangential component of the elastically scattered wavevector, while its normal component is equal but of opposite sign to that of the reflected wave. The construction can be repeated for any of the reciprocal vectors on the rod, denoting that reflection occurs at any angle of incidence.

Let us now consider the boundaries of the Brillouin zones which are due to the other rods of the reciprocal lattice. Every reciprocal vector is again bisected with a plane, as shown for one rod in Fig. 4(*b*). The planes form continuous envelopes. The intersections of the envelopes with the plane of the projection are confocal parabolas. The origin of the reciprocal lattice is their common focus, while the rods of the reciprocal lattice are their directrices (recall the definition for a parabola as a curve of equal distance between a point and a line). The parabolas extend in and out of the plane of the projection to form infinite parabolic surfaces. The equation of the parabolic surface that arises from the *hk* rod of the reciprocal lattice ($\mathbf{g}_{hk} = h\mathbf{a}^* + k\mathbf{b}^*$) can be expressed in terms of the components of the wave vector that are tangential ($\mathbf{k}_{0t}$) and normal ($\mathbf{k}_{0n}$) to the 2D real lattice [their projections to the plane of the drawing are denoted in Fig. 4(*b*)]:

$$\mathbf{k}_{0t}^2 + \mathbf{k}_{0n}^2 = \mathbf{k}_0^2 \tag{2}$$

$$\mathbf{k}_0^2 = \mathbf{k}^2 = (\mathbf{k}_{0t} - \mathbf{g}_{hk})^2 \tag{3}$$

$$\mathbf{k}_{0n}^2 = \mathbf{g}_{hk}^2 - 2\mathbf{g}_{hk} \cdot \mathbf{k}_{0t}. \tag{4}$$

Any wavevector starting at the origin of the reciprocal lattice and ending on one of these surfaces can be scattered elastically into a direction parallel to the 2D real lattice and *vice versa.* Because of this, the parabolic boundaries of the Brillouin zones can be of special interest.

We could now define *K* lines of 2D real lattices as directions given by the intersections of the described BZ boundaries with the sphere of reflections. Owing to the much less restrictive conditions than in the 3D case, the *K* lines of a true 2D lattice would yield an increased but mainly continuous background. The intersections of the sphere with the parabolic boundaries would be the only distinct features of the *K* map.

The experimental observations of the '2D *K* lines' are limited by the fact that the crystal samples used for electron and X-ray diffraction are always three-dimensional. A 2D real lattice is usually associated with surface-sensitive diffraction techniques, and in the case of LEED it is attributed to the small energy of the incident electrons, while in RHEED it is due to the grazing angle of incidence of the high-energy electrons. But, in both cases, the experimental patterns always show contributions from the bulk of the crystal, and in order to distinguish between the surface and the bulk features, proper dynamical calculations are needed when the surface has the same periodicity as the bulk. Thus, reconstructed surfaces would be the closest to the ideal free-standing 2D lattice for qualitative experimental studies of the geometry of the 2D Kikuchi lines. Channeling would give an additional case when the 3D crystal could diffract as an effective 2D lattice. We will treat the two cases in the following sections.

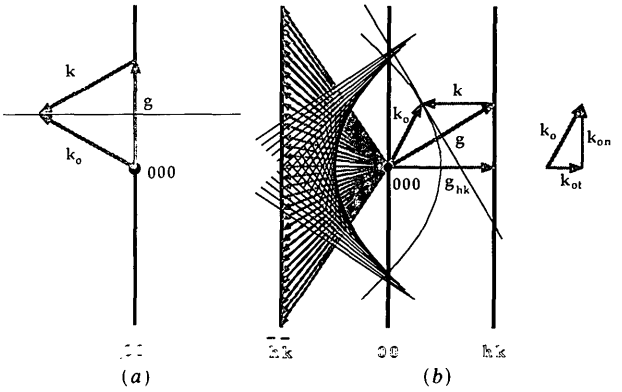

Fig. 4. Construction of the three-dimensional Brillouin zone boundaries for a two-dimensional lattice. (*a*) The planes bisecting the vectors of the 00 rod specify the reflection conditions for the 2D real lattice. (*b*) The envelopes of the planes that bisect the reciprocal vectors of the non-zero rods are parabolic surfaces. They define the condititions for elastic scattering into or out of the plane of the 2D lattice (when the incident or the scattered wavevector is parallel to the 2D lattice).

3.2. *Parabolas in RHEED patterns due to surface reconstructions*

The exact geometry of the K lines of true 2D lattices should be obtained by intersecting the sphere of reflections with the parabolic BZ boundaries of (4) and by considering the shape of the diffraction screen. For high-energy electrons (*i.e.* large radius of the sphere), the parabolas constructed in Fig. 4(b) are a good approximation for the experimental 2D K lines recorded on flat screens.

The diffraction experiments with surface reconstructions have in general been limited to UHV environments. They have been performed with parallel illumination and recorded with exposure times optimized to display the Bragg spots or rods. Because of this, the survey of the K lines in the published RHEED patterns did not reveal parabolas which are due to the surface periodicity. A hint of their existence can be obtained from the shape of the surface reconstruction spots in Fig. 1 of Ichikawa & Ino (1984).

Recently in our laboratory we have discovered a $(3^{1/2}\times 3^{1/2})R\ 30°$ reconstruction on the (111) surface of MgO which had been annealed at high temperature in oxygen atmosphere. The details of the surface preparation and characterization will be described elsewhere (Crozier, Gajdardziska-Josifovska & Cowley, 1990). For the purpose of this paper it is only important that the reconstruction is stable in air and provides a test 2D sample for diffraction experiments in conventional electron microscopes.

A reflection election microscope (REM) image of the MgO (111) surface and the RHEED patterns of the $\langle 2\bar{1}\bar{1}\rangle$ zone axis are shown in Fig. 5. The selected area patterns obtained for larger incident angle (Fig. 5b) and grazing incidence (Fig. 5c) show only bulk K lines (owing to the relatively low efficiency of the inelastic scattering as a sole provider of wide-angle coherent illumination). The intensity of the K lines is increased in the convergent-beam RHEED pattern shown in Fig. 5(d) in which two pairs of surface parabolas are clearly visible. The parabolas are smooth and continuous, as opposed to the more broken shape of the bulk parabola. Their positions and forms are as predicted in the geometrical construction of Fig. 4(b) with added refraction at the surface.

3.3. *Parabolas in THEED and RHEED patterns due to channeling*

Two qualitative conditions need to be met to attain channeling of electrons along or parallel to crystal planes. Firstly, a beam has to be excited whose wavevector is parallel or nearly parallel to a crystallographic plane (the energy of the component normal to the plane becomes very small). Secondly, the beam has to be trapped by the effective potential of the crystal plane (this makes the scattering from the individual parallel planes incoherent). For the channeled electrons, the 3D crystal would look like a collection of independent 2D lattices. The possible directions for elastic scattering out of each of the channeling planes would be defined by the parabolic BZ boundaries of 2D lattices. In the experimental HEED patterns, a band of confocal parabolas should arise from each crystal plane along which channeling occurs. The focus of all the parabolas that belong to a crystal zone would be on the zone axis. The 3D K bands of the channeling planes should be observed simultaneously with the 2D K bands of parabolas

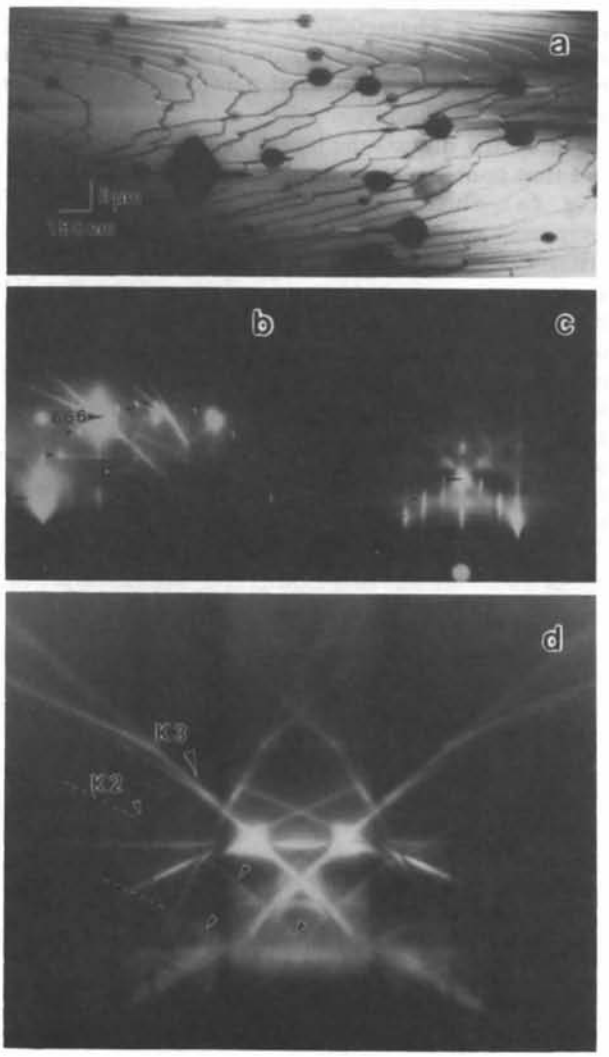

Fig. 5. Experimental REM image (a) and RHEED patterns from a $\langle 2\bar{1}\bar{1}\rangle$ zone axis of the $(3^{1/2}\times 3^{1/2})R\ 30°$ (111) surface of MgO recorded with: (b) parallel illumination at larger incident angle which was used for imaging; (c) parallel illumination at grazing incident angle; (d) convergent-beam illumination at grazing incident angle. The small arrows point to surface features in the diffraction patterns, the most important of which are the $K2$ parabolas in (d).

because for most of the incident-beam directions the crystal remains three-dimensional. The 3D K band of a crystallographic plane should be centered on the axis of symmetry of its band of parabolas. The 3D K lines arising from the other planes of the zone would be tangential to the parabolas. In the rest of this section we will attempt to unify the experimental observations and the previous explanations of the parabolas within the simple model of planar channeling followed by 2D diffraction.

The textbook definition of the parabolas in the THEED patterns is that they are envelopes of the 3D K lines (*e.g.* Hirsch *et al.*, 1977). This description is geometrically correct [recall Fig. 4(*b*) and perform the construction for a discrete set of points instead of continuous rods], but it has to call for dynamical diffraction effects to explain why continuous parabolas are actually observed in the experimental patterns (James, Bird & Wright, 1989).

For the parabolas obtained from 3D samples we would argue that the two different explanations: (i) 3D lattice with geometry defined by dynamical diffraction; and (ii) channeling with geometry obtained from kinematical conditions for a 2D lattice; could be treated as two equivalent models for the same phenomenon. In essence, the crystal planes which have deep potential wells with planar channeling states [see Gemmell (1974) for equations for channeling states] would also cause strong dynamical diffraction effects. The dynamical theory of electron diffraction is the only developed treatment which should be used to calculate the intensities of the parabolas, but the addition of a kinematical description for the HEED parabolas should prove useful for qualitative considerations. Namely, the geometry of most of the important features in the electron diffraction patterns can be understood from kinematical arguments, and the parabolas need not be an exception.

In the previous works dealing with the geometry of surface channeling (Ichimiya, Kambe & Lehmpfuhl, 1980; Lehmpfuhl & Dowell, 1986; Peng & Cowley, 1987), the parabolas were described as projected centers of Ewald spheres. This geometrical interpretation of the surface parabolas in the convergent-beam RHEED patterns is based on the conventional Ewald-sphere construction for elastic scattering in which the convergent beam is represented by a range of Ewald spheres. When each of those spheres is tangent to one rod of the reciprocal lattice, the projected centers of the Ewald spheres trace a parabola (Fig. 6) described by the equation

$$\mathbf{k}_{0n}^2 = \mathbf{g}_{hk}^2 + 2\mathbf{g}_{hk} \cdot \mathbf{k}_{0t} \qquad (5)$$

[the notation is modified to correspond to our notation in (4)].

Let us discuss the similarities and the differences between Fig. 6 and our Fig. 4(*b*). The parabolas in both geometries arise from the effective 2D nature of the real lattice. The geometry of Ichimiya, Kambe & Lehmpfuhl (1980) refers to the origin of the reciprocal lattice which is fixed to the incident-beam direction, while our parabolic Brillouin zone boundaries are specified with respect to the origin of the reciprocal lattice which is fixed to the crystal. This difference in the coordinate systems results in different signs of the dot products in (4) and (5) which are otherwise equivalent. The choice of the representation should only depend on the preferences of the reader, since they both give identical conclusions about the elastic scattering processes from a 2D real lattice. The advantage of the Brillouin zones approach (with only one sphere centered at the origin of the reciprocal lattice fixed to the crystal) could come from its direct correspondence to the experimentally observed diffraction patterns [*i.e.* projected centers of Ewald spheres are not associated with observable intensities, yet the parabolas that they trace are present in the HEED patterns; in addition, the impression from Fig. 6 is that the surface beam which is excited is on the outer side of the relevant parabola, while in the experimental patterns shown by Gajdardziska-Josifovska & Cowley (1989) the surface channeled beam is on the inner side of the parabola, as drawn in Fig. 4(*b*)].

The full geometrical description of an experimental THEED or RHEED pattern with channeling on some of the crystal planes would involve plotting of 3D and 2D K lines which are fixed to the crystal, and Bragg spots which are fixed to the incident beam (Gajdardziska-Josifovska & Cowley, 1989). In the RHEED case, the refraction effects at the surface need to be introduced as well (Peng & Cowley, 1987).

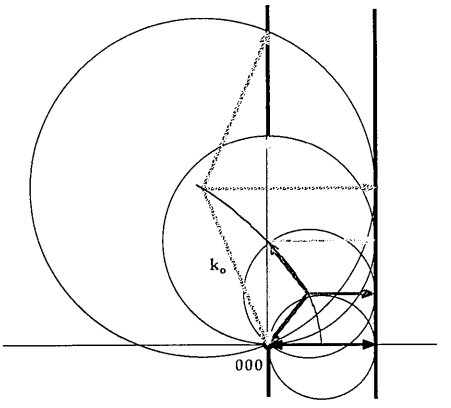

Fig. 6. The RHEED parabolas were explained as projected centers of Ewald spheres under angles of incidence when the spheres are tangent to the reciprocal-lattice rods (adapted from Ichimiya, Kambe & Lehmpfuhl, 1980). This geometry is equivalent to the geometry of Fig. 4(*b*).

Detailed studies of the various surface and bulk channeling cases will be described elsewhere.

3.4. *K*2 *lines in LEED patterns*

De Bersuder (1968) was the first to observe a new type of Kikuchi lines which appeared simultaneously with the ordinary (3D) Kikuchi lines in the LEED patterns from Al (001) surface. He related them to the two-dimensional nature of the surface, and called them $K2$ lines. The geometry of the experimental $K2$ lines (reproduced in Fig. 7*a*) was explained by intersections of the Ewald sphere centered at the origin of the reciprocal lattice with cylinders of radius $1/\lambda$ whose axes are the rods of the reciprocal lattice. No physical arguments were given to explain the meaning of the cylinders, but the proposed construction (shown in perspective in Fig. 7*b*) appears to agree with the experiment. De Bersuder suggested that the mechanism responsible for the $K2$ lines is analogous to the surface resonance effect. The supporting evidence for the connection between the $K2$ lines and the resonance effects in LEED has been reviewed by McRae (1979), together with the discussion that the surface resonance effects in LEED should be analogous to those in RHEED. Because of this we would like to apply the Brillouin zones of 2D real lattices to the LEED case in order to provide a consistent physical and geometrical explanation for the $K2$ lines and the HEED parabolas.

We could argue again that the lattice would be truly two-dimensional only to the electrons with wavevectors parallel to the surface which are trapped by the surface resonance states. The elastic scattering out of the surface plane would then be governed by the parabolic boundaries of the 2D Brillouin zones given by (4). The only LEED specific parameters would be the much smaller radius of the Ewald sphere, and the usual top view of the surface (as opposed to the grazing angle of view in RHEED). The intersection of the sphere of reflections [centered at the origin of the reciprocal lattice and having the same radius as the sphere in Fig. 7(*b*)] with one of the parabolic surfaces is presented in Fig. 7(*c*).

The 2D K line of Fig. 7(*c*) looks like the experimental lines of Fig. 7(*a*), but it also resembles the line of Fig. 7(*b*). Elementary derivations can show that the intersection of a sphere (centered at the origin: $x^2+y^2+z^2=\lambda^{-2}$) with a parabolic surface (*i.e.* due to the $h0$ rod: $z^2=g_{h0}^2-2g_{h0}x$) is a cylinder $[(x-g_{h0})^2+y^2=(\lambda)^{-2}$, with axis on the $h0$ rod]. Thus the two geometries are equivalent, and one could also think of the parabolas in the HEED patterns as intersections of a large sphere with large cylinders. The advantage of the Brillouin-zone scheme would come from its generality and the familiarity of the involved physical concepts.

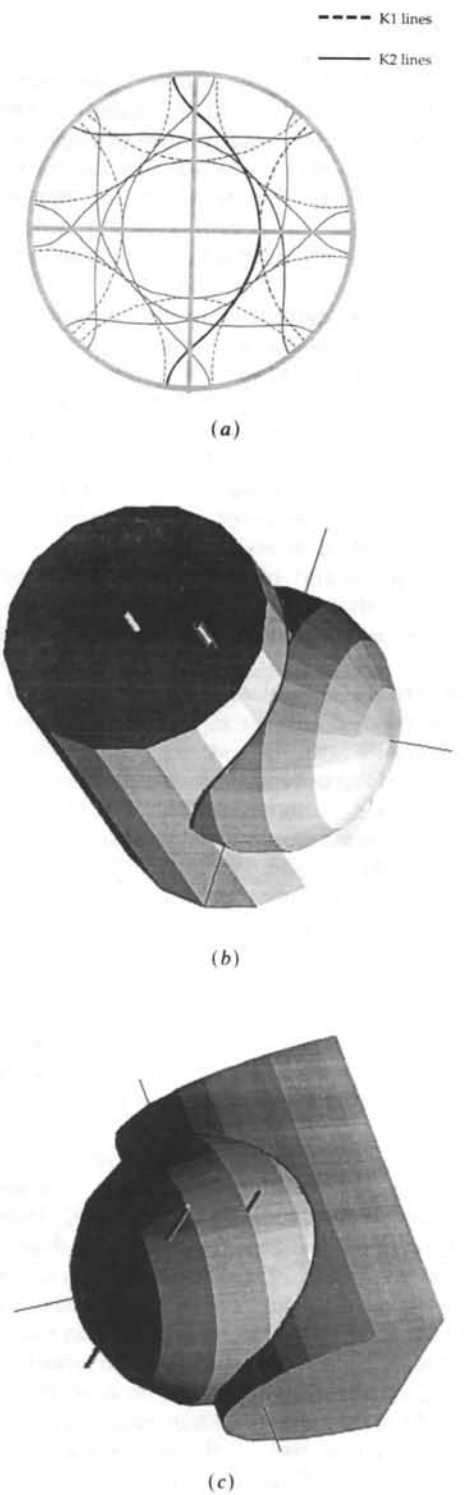

Fig. 7. (*a*) Stereographic projection of LEED K_2 and K_1 lines from Al (100) surface (after De Bersuder, 1968). (*b*) Geometry of $K2$ lines was explained by De Bersuder as the intersection of a sphere (centered at the origin of the reciprocal lattice) with a cylinder of the same radius whose axis is a rod of the reciprocal lattice. (*c*) The intersection of the sphere of reflections with the parabolic Brillouin zone boundaries also reproduces the correct geometry of the $K2$ lines.

4. Brillouin zones of 1D real lattices

4.1. *Construction and properties*

The reciprocal lattice of a 1D real lattice is made of equidistant planes which are othogonal to the line of the real lattice. Owing to the azimuthal symmetry about the string of the real lattice, the projections of the reciprocal lattice on any planes that are parallel to the real lattice are identical. These projections are made of rods, and the constructions for the 2D lattices shown in Fig. 4 can be used to explain the Brillouin zones of the 1D lattice.

The boundaries that arise from the plane that contains the origin of the reciprocal lattice describe the reflection of the waves which are incident at an arbitrary angle to the 1D lattice. The boundaries that arise from the other planes of the reciprocal lattice can be obtained by rotating Fig. 4(*b*) about the horizontal axis of symmetry. The continuous envelopes in the 1D case are confocal paraboloids of revolution (Fig. 8). The focal point is again the reciprocal-lattice origin. The points on the surfaces of the paraboloids specify the directions for elastic scattering of waves with incident wavevectors that are parallel to the 1D string of scatterers and *vice versa*. Equation (4) can be modified to describe the paraboloids by replacing $\mathbf{g}_{hk}$ with its 1D equivalent $\mathbf{g}_h$ (where $\mathbf{g}_h = h\mathbf{a}^*$) and by making it scalar (*i.e.* the dot product is not necessary since now $\mathbf{k}_{0t}$ is the component of the wavevector tangential to the 1D lattice and thus parallel to $\mathbf{g}_h$):

$$k_{0n}^2 = g_h^2 - 2g_h k_{0t}. \tag{6}$$

4.2. *1D K lines and axial channeling*

If the real lattice is an ideal 1D lattice, then all the boundaries of the '1D' Brillouin zones need to be considered. In the actual experiments the real lattice is 3D (bulk crystals) or 2D (reconstructed surfaces) and the paraboloids of revolution gain special importance because they specify the directions for elastic scattering of the axially channeled waves. The intersections of these paraboloids of revolution with the sphere of reflections should produce the '1D *K* lines'. Since the focus of the paraboloids and the center of the sphere coincide, the intersections are circles which are centered about the crystallographic direction of the channeling rows of atoms (Fig. 9). The scattered wavevectors, which start at the center of the sphere and end on those circles, form cones with semiapex angles $\varphi_n = \cos^{-1}(1 - ng_h\lambda)$. The intersections of the cones with the diffraction screen would define the actual shape of the experimentally observed 1D *K* lines.

In the HEED patterns the small-angle approximation can be applied to the semiapex angles of the cones to give $\varphi_n = (2ng_h\lambda)^{1/2}$. The screen is flat and the conical sections give circles (when the channeling row of atoms is oriented perpendicular to the screen) or ellipses (for off-axis tilts of the crystal, or due to the refraction effects in RHEED). In the practical cases the eccentricity of the ellipses is small and for further discussion we will regard the 1D HEED *K* lines to be circles.

When the incident beam is parallel to the channeling row of atoms, the high-order Laue zone (HOLZ) Bragg spots lie on the 1D *K* circles. This is a typical configuration in the axial channeling THEED experiments (Ichimiya & Lehmpfuhl, 1978), but the attention in those works has concentrated on the intensities of the *K* pattern close to the zone axis and the *K* circles which are a direct consequence of the axial channeling have not been studied. The circles in the THEED patterns were described as envelopes of parabolas, just as the parabolas were understood as envelopes of Kikuchi lines (*e.g.* Hirsch *et al.*, 1977).

In the RHEED patterns the continuous semicircles were noted very early, and were associated with electron channeling along rows of atoms on the crystal surface (Emslie, 1934). In the more modern UHV experiments with Si (111) surfaces, semicircles were observed which correspond to the 7×7 surface periodicity (*e.g.* Ino, 1977). Recently, Yao & Cowley

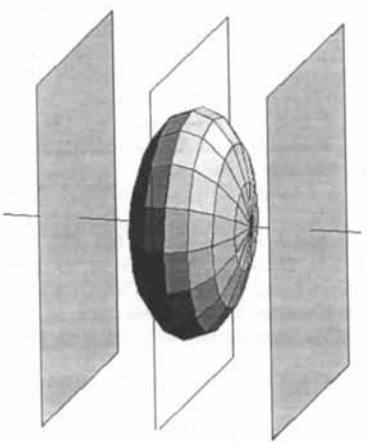

Fig. 8. The Brillouin zone boundaries which specify the scattering of the waves that propagate parallel to the 1D real lattice are paraboloids of revolution. This figure illustrates parts of the paraboloids which arise from the two reciprocal-lattice planes which are closest to the origin of the reciprocal space.

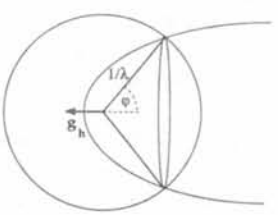

Fig. 9. The intersection of the sphere of reflections with the paraboloid of revolution (arising from the $\mathbf{g}_h$ vector) is a circle. The scattered vectors form a cone with a semiapex angle $\varphi = \cos^{-1}(1 - g_h\lambda)$.

(1989) compared the RHEED and THEED patterns of several crystals and concluded that the circles in both cases are due to axial channeling. The illumination in the RHEED configuration is tilted and the circles are separated from the HOLZ Bragg spots. This separation was measured by Yao & Cowley to obtain information about the axial channeling energy levels.

In the LEED experiments the cones which correspond to the 1D K lines intersect the semispherical diffraction screen in circles or segments of circles. Thus, the geometry of the 1D K lines is identical to the geometry of the 3D K lines, but the position of the circle arising from the 1D reciprocal-lattice vector $\mathbf{g}_h$ should differ from the position of the corresponding 3D circle arising from the vector g_{h00} [*i.e.* the semiapex angles of the two cones that give the 1D circle and the 3D circle are different: $\varphi_{1D} = \cos^{-1}(1 - g_h\lambda)$; $\varphi_{3D} = \cos^{-1}(g_{h00}\lambda/2)$].

LEED circular arcs which could not be explained as 3D K lines were first observed by Germer & Chang (1966) and were associated with 1D diffraction. They were called $K1$ lines by De Bersuder (1968) who discussed their relation with the $K2$ lines. $K1$ lines have not gained attention in the LEED surface resonance studies.

5. Concluding remarks

A general explanation of the geometry of the HEED and LEED K patterns has been obtained by developing the complete geometry of the Brillouin zones, and by intersecting the Brillouin zone boundaries with the sphere of reflections.

Of all the boundaries of the Brillouin zones of 2D lattices, the parabolic bounding surfaces are shown to describe the elastic scattering from the crystal planes at channeling conditions. The intersections of these surfaces with the sphere of reflections are shown to give the experimentally observed parabolas in the HEED patterns, and the $K2$ lines of the LEED patterns. In both cases, the planar (surface) channeling appears to be the necessary primary event for obtaining 2D K lines in the diffraction pattern of a 3D crystal. Thus, the presence of the 2D K lines is an unambiguous sign that the corresponding crystal planes possess channeling quantum states at the given crystal orientation and for the used energy of incident electrons. This simple model of channeling followed by 2D diffraction unifies the previous numerous but rather diverging descriptions of parabolas, $K2$ lines and channeling.

Additional support for the proposed description is obtained from the diffraction experiments with a $(3^{1/2} \times 3^{1/2})R\ 30°$ MgO (111) surface which serves as a test 2D sample. In the CBED RHEED patterns we observe parabolas which correspond to the surface periodicity and which yield the first experimental evidence that the parabolas are K lines of 2D lattices.

The axial channeling followed by diffraction from the effective 1D lattice gives circles in the K patterns. The geometry of this case may also be described in terms of the relevant Brillouin zone boundaries which are shown to be paraboloids of revolution.

The full description of the Brillouin zones of 2D and 1D lattices should be of utmost importance in all the solid-state problems when the dimensionality of the crystal is reduced. The existence of 2D and 1D K lines in the diffraction patterns of 3D crystals suggests that similar effects should be observed for any angular resolved signals from '2D' and '1D' crystals.

The authors are grateful to Drs P. A. Crozier and M. R. McCartney for numerous discussions and their critical reading of the manuscript, and to Dr J. C. H. Spence for his generous donation of a large MgO crystal which enabled the experiments with the (111) surface.

This work was supported by DOE grant DE-FG02-86ER45228 and made use of the resources of the ASU materials electron microscope and the Facility for High Resolution Electron Microscopy, supported by NSF grant DMR-8611609.

References

CHADDERTON, L. T. (1970). *J. Appl. Cryst.* **3**, 429-465.
COWLEY, J. M. (1984). *Diffraction Physics*, pp. 315-318. Amsterdam: North-Holland.
CROZIER, P. A., GAJDARDZISKA-JOSIFOVSKA, M. & COWLEY, J. M. (1990). *J. Electron Microsc. Tech.* In preparation.
DE BERSUDER, L. (1968). *C. R. Acad. Sci. Ser. B*, **266**, 1489-1491.
EMSLIE, A. G. (1934). *Phys. Rev.* **45**, 43-46.
FAN, G. Y. (1989). *Proc. 47th Annual EMSA Meeting*, edited by G. W. BAILEY, pp. 52-53. San Francisco: San Francisco Press.
GAJDARDZISKA-JOSIFOVSKA, M. & COWLEY, J. M. (1989). *Proc. 47th Annual EMSA Meeting*, edited by G. W. BAILEY, pp. 498-499. San Francisco: San Francisco Press.
GEMMELL, D. S. (1974). *Rev. Mod. Phys.* **46**, 129-227.
GERMER, L. H. & CHANG, C. C. (1966). *Surf. Sci.* **4**, 498-501.
HIRSCH, M. A., HOWIE, A., NICHOLSON, R. B., PASHLEY, D. W. & WHELAN, M. J. (1977). *Electron Microscopy of Thin Crystals*, pp. 121-124. Malabar: Krieger.
ICHIKAWA, T. & INO, S. (1984). *Surf. Sci.* **136**, 267-284.
ICHIMIYA, A., KAMBE, K. & LEHMPFUHL, G. (1980). *J. Phys. Soc. Jpn*, **49**, 684-688.
ICHIMIYA, A. & LEHMPFUHL, G. (1978). *Z. Naturforsch Teil A*, **33**, 269-281.
INO, S. (1977). *Jpn. J. Appl. Phys.* **16**, 891-908.
JAMES, R., BIRD, D. M. & WRIGHT, A. G. (1989). *Inst. Phys. Conf. Ser.* No. 98, edited by P. J. GOODHEW & H. Y. ELDER, pp. 111-114. Reading: Eastern Press Ltd.
KITTEL, C. (1976). *Introduction to Solid State Physics*, p. 51. New York: John Wiley.
LEHMPFUHL, G. & DOWELL, W. C. T. (1986). *Acta Cryst.* A**42**, 569-577.
MCRAE, E. G. (1979). *Rev. Mod. Phys.* **51**, 541-568.
MIYAKE, S. & HAYAKAWA, K. (1970). *Acta Cryst.* A**26**, 60-70.
PENG, L.-M. & COWLEY, J. M. (1987). *J. Electron Microsc. Tech.* **6**, 43-53.
SPENCE, J. C. H. (1990). *Electron Diffraction Techniques*, edited by J. M. COWLEY, Ch. 8. Oxford Univ. Press. In the press.
YAO, N. & COWLEY, J. M. (1989). *Ultramicroscopy*, **31**, 149-157.